SLAC-PUB-16243

Strong Influence of Coadsorbate Interaction on CO Desorption Dynamics Probed by Ultrafast X-ray Spectroscopy and Ab Initio Simulations

H. Xin,[1,2] J. LaRue,[1] H. Öberg,[3] M. Beye,[1,4] M. Dell'Angela,[5] J. J. Turner,[6] J. Gladh,[3] M. L. Ng,[1] J. A. Sellberg,[1,4] S. Kaya,[1] G. Mercurio,[5] F. Hieke,[5] D. Nordlund,[7] W. F. Schlotter,[6] G. L. Dakovski,[6] M. P. Minitti,[6] A. Föhlisch,[4,8] M. Wolf,[9] W. Wurth,[5,10] H. Ogasawara,[7] J. K. Nørskov,[1,2] H. Öström,[3] L. G. M Pettersson,[3] A. Nilsson,[1,3,7] and F. Abild-Pedersen[1,*]

[1]*SUNCAT Center for Interface Science and Catalysis, SLAC National Accelerator Laboratory, 2575 Sand Hill Road, Menlo Park, CA 94025, USA*
[2]*SUNCAT Center for Interface Science and Catalysis, Department of Chemical Engineering, Stanford University, Stanford, CA 95305, USA*
[3]*Department of Physics, AlbaNova University Center, Stockholm University, SE-10691 Stockholm, Sweden*
[4]*Helmholtz Zentrum Berlin für Materialien und Energie GmbH, Albert-Einstein-Strasse 15, D-12489 Berlin, Germany*
[5]*University of Hamburg and Center for Free Electron Laser Science, Luruper Chausse 149, D-22761 Hamburg, Germany*
[6]*Linac Coherent Light Source, SLAC National Accelerator Laboratory, 2575 Sand Hill Road, Menlo Park, CA 94025, USA*
[7]*Stanford Synchrotron Radiation Lightsource, SLAC National Accelerator Laboratory, 2575 Sand Hill Road, Menlo Park, CA 94025, USA*
[8]*Fakultät für Physik und Astronomie, Universität Potsdam, Karl-Liebknecht-Strasse 24-25, 14476 Potsdam, Germany*
[9]*Fritz-Haber Institute of the Max-Planck-Society, Faradayweg 4-6, D-14195 Berlin, Germany*
[10]*DESY Photon Science, Notkestr. 85, 22607 Hamburg, Germany*

We show that coadsorbed oxygen atoms have a dramatic influence on the CO desorption dynamics from Ru(0001). In contrast to the precursor-mediated desorption mechanism on Ru(0001), the presence of surface oxygen modifies the electronic structure of Ru atoms such that CO desorption occurs predominantly via the direct pathway. This phenomenon is directly observed in an ultrafast pump-probe experiment using a soft x-ray free-electron laser to monitor the dynamic evolution of the valence electronic structure of the surface species. This is supported with the potential of mean force along the CO desorption path obtained from density-functional theory calculations. Charge density distribution and frozen-orbital analysis suggest that the oxygen-induced reduction of the Pauli repulsion, and consequent increase of the dative interaction between the CO 5σ and the charged Ru atom, is the electronic origin of the distinct desorption dynamics. *Ab initio* molecular dynamics simulations of CO desorption from Ru(0001) and oxygen-coadsorbed Ru(0001) provide further insights into the surface bond-breaking process.

PACS numbers: 31.15.A-,68.35.Ja,82.53.-k,82.20.-w, 82.40.-g,78.70.Dm

Desorption of molecules, or their fragments, from a surface into the gas phase represents the most fundamental bond-breaking step in heterogeneous catalysis [1–3]. In this process, the existence of a relatively short-lived and weakly-adsorbed precursor species has long been conjectured when interpreting measured kinetics [4–8]. Recently, this surface species has been directly observed with a soft x-ray free-electron laser using ultrafast pump-probe techniques [9, 10]. The spectroscopic identification of the precursor state rationalizes many phenomena in gas-surface interactions [4–8] and underpins our fundamental understanding of the kinetics of elementary surface reactions. In heterogeneous catalytic processes, many different species or promoters exist on the surface that can influence each other through adsorbate-adsorbate interactions [11]. Effects of the coadsorbate interaction on desorption dynamics have, however, largely been unexplored and their role in the correlated chemical environment is presently still poorly understood [11–13].

In this Letter, we present experimental and theoretical evidence of a strong influence of coadsorbed oxygen atoms on the mechanistic aspects of CO desorption from Ru(0001). Using femtosecond time-resolved x-ray absorption spectroscopy (XAS) with an x-ray free-electron laser and density-functional theory (DFT) calculations, we show that CO desorption occurs via the direct pathway on oxygen-coadsorbed Ru(0001) rather than the precursor-mediated pathway found on bare Ru(0001) [9, 10]. The substrate-mediated adsorbate-adsorbate interaction, dominated by the oxygen-induced reduction of the Pauli repulsion and consequent increase of the dative interaction between the CO 5σ and the charged Ru atom, is identified as the underlying force that steers the desorbing molecules along the favored pathway. *Ab initio* molecular dynamics (AIMD) simulations support the proposed mechanism and provide further insights into the

This material is based upon work supported by the U.S. Department of Energy, Office of Science, Office of Basic Energy Sciences, under Contract No. DE-AC02-76SF00515 and LDRD.

surface bond-breaking process.

The experiments were performed at the Linac Coherent Light Source (LCLS) facility that provides intense, coherent femtosecond x-ray pulses [14]. The Ru(0001) single crystal was cleaned with standard sputtering-annealing procedures and was kept at 300 K [15]. A saturated (∼0.66 ML) CO/Ru(0001) adlayer was prepared with the background CO pressure at 1.0×10^{-8} torr. To investigate effects of coadsorbed oxygen atoms on CO desorption, a 2O-CO/Ru(0001) honeycomb surface structure with 1/2 ML O and 1/4 ML CO was prepared (see Fig. S1, S2 and S5 for modeled surface structures) [16]. Optical laser pulses initiate surface reactions, which for CO/Ru(0001) lead to desorption [9, 10, 17–19] and for 2O-CO/Ru(0001) include both CO desorption and a minor contribution from oxidation to CO_2 [20–22]. The temperature profile of the electron and phonon subsystems induced by ultrafast optical lasers can be described using the two-temperature model [16, 24, 25]. The absorption of visible photons in a metal substrate first gives rise to a non-equilibrium distribution of hot electrons which thermalizes on a time scale of a couple of hundred fs [23] into a quasi-equilibrium distribution with a peak temperature of several thousand K. The hot electrons then couple to phonon modes of the substrate and surface species and thermal equilibrium is reached within a couple of ps [24, 25]. The valence electronic structure of CO species was monitored in real time through resonant O 1s to $2\pi^*$ (O K-edge) excitation with a soft x-ray pulse. The involvement of the O 1s core level makes this an atom-specific and local probe of the electronic structure in contrast to a valence spectroscopy that would measure the extended band structure. Space-charge effects are furthermore avoided through measuring fluorescence yield.

Fig. 1 shows the measured O K-edge XAS spectra of CO/Ru(0001) before and 12 ps after the 400 nm optical laser pump at absorbed fluence 140 J/m^2 with 170 fs duration (experimental details and intermediate time steps are given in the Supplementary Material of ref. [9]). The O K-edge XAS probes the distribution of unoccupied CO $2\tilde{\pi}^*$ states where the tilde is used to denote the modified adsorbate electronic structure compared to the gas phase. The spectrum at negative delay, which corresponds to the static configuration before the optical laser pump, has the characteristic CO $2\tilde{\pi}^*$ peak at 533.5 eV. At 12 ps probe delay, when electron and phonon subsystems are thermally equilibrated at 1500-2000 K (see Fig. S3), a blue-shift of the CO $2\tilde{\pi}^*$ peak towards the gas phase and an enhancement in its intensity was observed. The nature of this peak is consistent with a substantial population (∼30%) of a weakly-adsorbed precursor species prior to desorption [9, 10]. For 2O-CO/Ru(0001) before the optical laser pump, the CO $2\tilde{\pi}^*$ peak is found at 533.3 eV. At 13 ps probe delay, on a similar time scale as for the CO/Ru(0001) case above, this peak instead broadens and

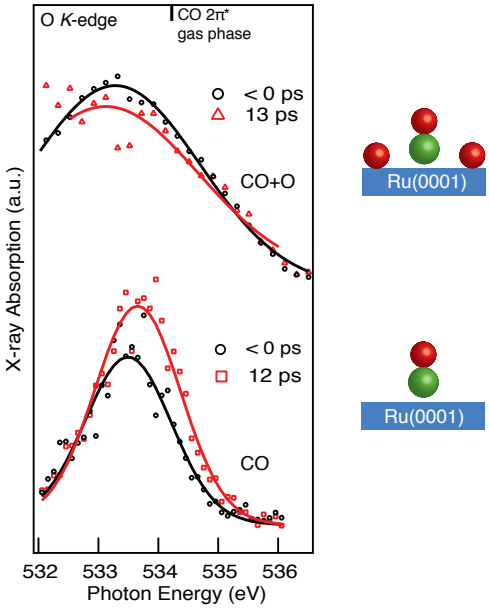

FIG. 1: O K-edge XAS spectra showing the $2\pi^*$ resonance of CO/Ru(0001) and 2O-CO/Ru(0001) measured before and ∼10 ps after the optical laser pump.

shifts slightly down in energy. This is a signature of hot CO molecules migrating from atop towards bridge or hollow sites, consistent with measurements of CO/Ru(0001) at short (< 1 ps) probe delays when adsorbed CO is not yet pumped into the precursor state [9, 10]. The time evolution of this species has been related to the formation of transition-state species as the molecules that do not desorb undergo repeated attempts to form CO_2 [26]. The unanticipated observation is that the precursor state for CO desorption, which exists on Ru(0001) [9, 10] and many other transition-metal surfaces [6–8], vanishes on 2O-CO/Ru(0001). This is not due to oxidation of CO to CO_2 since ∼90% of the products desorbing from the surface are CO molecules [20, 21]. This instead suggests that CO desorption from 2O-CO/Ru(0001) occurs via the direct rather than the precursor-mediated pathway.

To understand the observed dynamics of CO desorption, density-functional theory calculations with the BEEF-vdW [27] exchange-correlation functional were used to probe the energetics of CO along the desorption path above Ru(0001) [16]. Fig. 2 shows the free energy surface of CO desorption from CO/Ru(0001) and 2O-CO/Ru(0001) at 0 K and 2000 K. The reaction path is defined as the distance from the center-of-mass of CO to the Ru surface plane. The free energy, $G(s)$, along the reaction coordinate, s, was calculated using the potential of mean force approach [4, 5] that defines $G(s)$ as,

$$G(s) = V_0(s) - k_B T \sum_{\mathbf{q}\perp\mathbf{s}} \ln \int \exp[-V(q,s)/k_B T] dq \quad (1)$$

where k_B is Boltzmann's constant, T is the temperature,

q represents all degrees of freedom of CO that are orthogonal to s. $V_0(s)$ is the minimum potential energy path and $V(q,s)$ is the interaction potential for mode q relative to $V_0(s)$. This approach essentially takes into account the entropic contributions from all thermally accessible modes of adsorbed CO including frustrated translations and rotations [16]; at elevated temperatures the anharmonicity of the potential energy surface leads to significant contributions to the partition function and thus to the entropy [28].

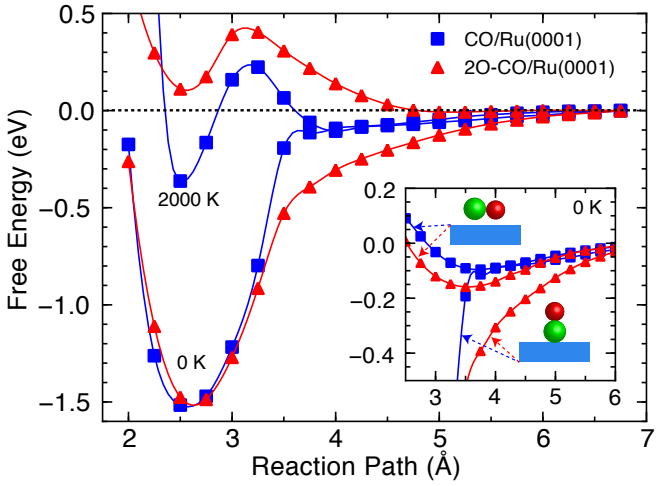

FIG. 2: The free energy surface for CO desorption from CO/Ru(0001) and 2O-CO/Ru(0001) at 0 K and 2000 K. The inset shows the potential energy surface of a CO molecule in perpendicular and parallel configuration on Ru(0001) and 2O-CO/Ru(0001).

The minimum of the potential well at 0 K represents the chemisorption energy of CO at the atop site of Ru(0001) that was calculated to be -1.52 eV versus the experimental value of -1.6 eV [13]. The bonding at the equilibrium geometry is characterized by the formation of a π-bond enabled by mixing CO 1π and $2\pi^*$ to partially break the internal π-bond while the σ-interaction is repulsive [29, 30]. Coadsorption of atomic oxygen (1/2 ML) on Ru(0001) has a small effect on the calculated equilibrium bond strength [31] confirmed by only a minor ($\sim$0.2 eV) destabilization observed experimentally [32]. At longer distances ($d_{\text{CO-Ru}} > 3.5$ Å), the interaction of CO with the Ru(0001) surface becomes very weak. We define this region as the precursor region where the CO molecule might get trapped prior to desorption from Ru(0001) [9, 10]. Interestingly, as atomic oxygen is coadsorbed on the surface, the CO-Ru interaction becomes much more attractive within this region. For example, at 3.75 Å above the surface, the CO-Ru bond on 2O-CO/Ru(0001) is 0.3 eV (a factor of 3) stronger than that on CO/Ru(0001).

At elevated temperatures (see Fig. 2 and Fig. S4), a temperature-induced entropic barrier for desorption appears at 3.25 Å above the surface separating the chemisorbed state and the gas phase. This is due to the reduced entropy of chemisorbed species compared to that of CO molecules far away from the surface. For CO/Ru(0001), a shallow free energy well with a minimum $\sim$-0.1 eV emerges within the precursor region that accommodates precursor CO molecules prior to desorption or adsorption. At 2000 K, the chemisorbed and physisorbed states both have comparable free energies (within $\sim 2k_BT$). This is consistent with the measurement shown in Fig. 1 where a substantial amount of desorbing CO molecules is pumped into the precursor state within 10 ps [9, 10]. In contrast, there is no local minimum in the precursor region for CO desorption from 2O-CO/Ru(0001). The CO molecules on 2O-CO/Ru(0001) that cross the barrier would energetically go into the gas phase without being transiently trapped, i.e., CO most likely desorbs through the direct pathway. This is fully consistent with the interpretation of the spectra and the subsequent dynamics of CO desorption shown in Fig. 1.

This raises the apparent question regarding the underlying cause of the dramatic difference in the free energy surface that governs CO desorption dynamics. To tackle this question, we show in the inset of Fig. 2 the potential energy of CO in perpendicular and parallel configuration on Ru(0001) and 2O-CO/Ru(0001). For CO/Ru(0001), these two configurations have nearly identical energies within the precursor region, suggesting that an adsorbed CO molecule has very soft rotational modes similar to CO molecules far away from the surface. Increasing the system temperature will not change the free energy of adsorbed CO in the precursor region relative to gas phase, thus it leads to a second minimum above the surface with an entropic barrier separating it from the chemisorbed state. As oxygen atoms are coadsorbed on the surface, the perpendicular mode becomes more energetically favorable than the parallel configuration in this region ($\sim$0.2 eV more exothermic at 3.75 Å above the surface). This indicates that the rotational mode of CO molecules within the precursor region on 2O-CO/Ru(0001) is significantly more constrained compared to that of CO molecules far away from the surface. As a consequence, the relative free energy of CO molecules above the 2O-CO/Ru(0001) surface shifts up at elevated temperatures, leaving no local minimum within the precursor region; this conclusion holds also for disordered O adsorption [16]. The fundamental question that remains is: what is the electronic origin of the distinct energy profiles that result in the observed difference in the CO desorption dynamics?

To answer this question, the CO-induced charge density difference (CDD) is shown in Fig. 3(a) and (b) for CO within the precursor region (3.75 Å above the surface as an example). The CDD is calculated by subtracting the charge density of CO and the system without CO from the combined system at fixed atomic positions.

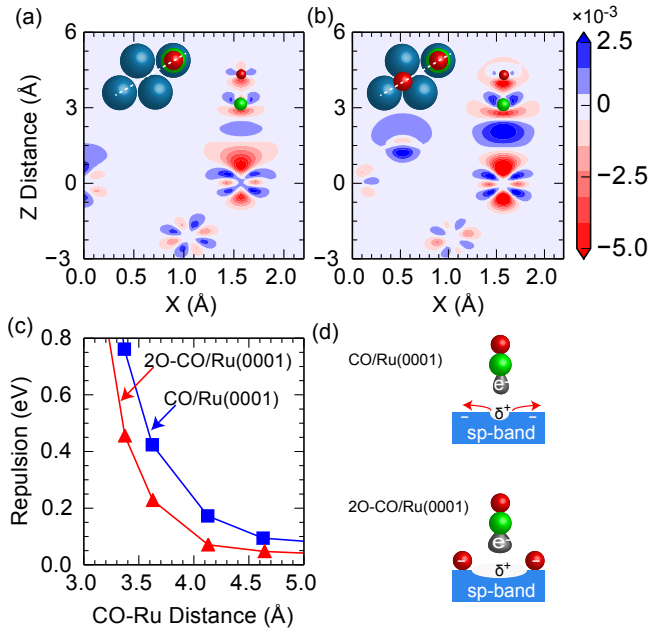

FIG. 3: Electronic origin of O-induced long-ranged interactions of CO (3.75 Å) on Ru(0001). CO induced charge density difference on (a) CO/Ru(0001) and (b) 2O-CO/Ru(0001). Insets show the direction cutting through CO molecules. (c) Repulsive interaction energy between CO with Ru(0001) and 2O/Ru(0001) obtained from frozen-orbital calculations. (d) Cartoon illustration of the interaction of the CO 5σ orbital with the *sp*-band of Ru surface atoms for CO/Ru(0001) and 2O-CO/Ru(0001).

Here we focus on the region between CO and Ru along the axis where clearly there is additional charge accumulation between the C and the Ru atom for CO interacting with O/Ru (Fig. 3b) in comparison to bare Ru (Fig. 3a). Based on symmetry arguments this indicates substantial changes in the σ-interaction. Although it has been shown that the CO σ-orbitals have a repulsive interaction with the Ru surface at the equilibrium distance [3, 12, 30, 33], the picture could be different at the longer distances in the precursor region. The additional charge accumulation between the C and the Ru atom results from an attractive electrostatic interaction with CO 5σ density via a dative interaction that becomes more prominent on 2O-CO/Ru(0001) (Fig. 3b). The pulling of electron density away from the Ru site by coadsorbed oxygen makes Ru positively charged (see Fig. S6), leading to weaker Pauli repulsion and a stronger electrostatic attraction with the CO 5σ density. This mechanism is illustrated in Fig. 3(d).

To further quantify the energetics in the interaction, we have used a frozen-orbital approach [16] that only allows orbital orthogonalization and thus provides an estimation of the repulsive energy between interacting subunits [34]. Results in Fig. 3(c) show that there is a significant difference in the repulsive interaction of CO in the precursor region with the bare Ru(0001) compared to that with the 2O-CO/Ru(0001). The oxygen-induced reduction in repulsive energy (for example, 0.15 eV at 3.75 Å) partially accounts for the potential energy difference (0.3 eV at 3.75 Å) between CO/Ru(0001) and 2O-CO/Ru(0001) within the precursor region shown in Fig. 2. So we conclude that the energy difference of CO-Ru interaction in perpendicular bonding configuration on CO/Ru(0001) and 2O-CO/Ru(0001) within the precursor region is coming from both the oxygen-induced reduction of Pauli repulsion and a more effective resulting dative interaction between CO 5σ and the positively charged Ru atom. This mechanism also explains the much weaker bonding to the surface of CO molecules in parallel configuration (shown in the inset of Fig. 2) where both the Pauli repulsion and the electrostatic dative attraction become negligible. This unravels the underlying electronic origin of long-ranged interactions of CO on 2O-CO/Ru(0001) and provides a molecular orbital perspective into the dynamics of surface bond-breaking processes.

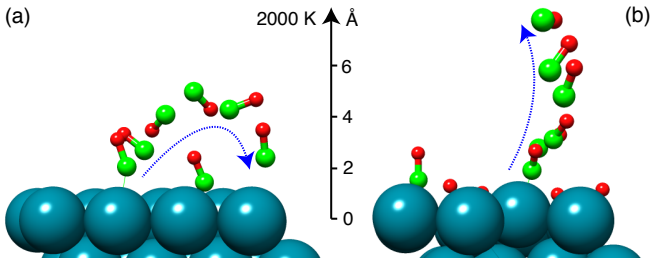

FIG. 4: Snapshots of CO desorption trajectories taken from AIMD simulations at 2000 K for (a) CO/Ru(0001) and (b) 2O-CO/Ru(0001).

To gain further insights into the CO desorption dynamics, we have performed AIMD simulations at 2000 K [16]. These are used to understand the mechanism of surface bond-breaking processes rather than to obtain detailed statistics, which would require many trajectories. We found that CO desorption on CO/Ru(0001) typically occurs on a longer time scale than that on the 2O-CO/Ru(0001) surface. This is consistent with the free energy barrier observed in Fig. 2. On both surfaces, the process is initiated by hot substrate phonons that collide with rotationally frustrated CO molecules, as seen in Fig. 4. On CO/Ru(0001), when CO desorbs, it can be transiently trapped in the precursor state (Fig. 4a). This is because the rotational modes of CO in the precursor region are very soft, such that the kinetic energy of CO molecules can be converted into rotation reducing the momentum in the direction of desorption. Subsequently CO can desorb, although with a slightly higher translational energy than that from 2O-CO/Ru(0001) due to prolonged coupling to hot surface phonons [19, 21]. For 2O-CO/Ru(0001), once CO crosses the barrier, the free energy becomes downhill and it will desorb directly, with-

out being trapped as seen in Fig. 4(b). This can be easily understood since the perpendicular mode of CO is much more favored over the parallel mode so that the desorbing molecule only couples weakly to the rotational modes, i.e., it would rather keep momentum in the direction of desorption without being trapped.

The dynamics of desorption processes of surface species has many important consequences on the outcome of catalytic reactions. For CO oxidation on Ru(0001), there is a direct competition between CO desorption and oxidation [21]. The presence of oxygen atoms makes the desorption step more facile with a smaller free energy barrier. Furthermore, the absence of a precursor state can be expected to reduce the probability that an incoming CO molecule adjusts its molecular reorientation through rotations in the precursor region and then finds vacant sites for adsorption or reacts with activated atomic oxygen to form CO_2.

In conclusion we use ultrafast pump-probe experimental measurements and state-of-the-art electronic structure calculations to demonstrate a dramatic influence by the coadsorbate interaction on the CO desorption dynamics from Ru(0001). We show that the free energy at the precursor region is dramatically influenced by entropy, where CO with coadsorbed O on Ru(0001) is more constrained than on Ru(0001) leaving no local precursor state prior to desorption at elevated temperatures. We found that the oxygen-induced reduction of the Pauli repulsion and increased electrostatic dative interaction between the CO 5σ and the positively charged Ru atom on 2O-CO/Ru(0001) drives the CO desorption via the direct desorption pathway instead of the precursor-mediated pathway. AIMD simulations further support the experimental observation and provide a microscopic view of surface bond-breaking processes. The fundamental insights gained here consolidate our understanding of surface chemical bonding and underline the importance of including coadsorbate interactions when unraveling dynamics of surface reactions.

This work is supported by the US Department of Energy, Basic Energy Science through the SUNCAT Center for Interface Science and Catalysis and the Swedish Research Council (VR). F.A.P. and H.O. also acknowledge the Department of Energy, Laboratory Directed Research and Development funding, under contract DE-AC02-76SF00515. MB acknowledges funding from the VolkswagenStiftung. Portions of this research were carried out on the SXR Instrument at the Linac Coherent Light Source (LCLS), a division of SLAC National Accelerator Laboratory and an Office of Science user facility operated by Stanford University for the U.S. Department of Energy. The SXR Instrument is funded by a consortium whose membership includes the LCLS, Stanford University through the Stanford Institute for Materials Energy Sciences (SIMES), Lawrence Berkeley National Laboratory (LBNL), University of Hamburg through the BMBF priority program FSP 301, and the Center for Free Electron Laser Science (CFEL). Some of the calculations were performed on resources provided by the Swedish National Infrastructure for Computing (SNIC) at the HPC2N center.

* Electronic address: abild@slac.stanford.edu

[1] G. Ertl, *Reactions at Solid Surfaces* (Wiley, Hoboken, N.J, 2009), 2nd ed.

[2] R. D. Muino and H. F. Busnengo, *Dynamics of Gas-Surface Interactions: Atomic-level Understanding of Scattering Processes at Surfaces* (Springer, New York, 2013), 2013th ed.

[3] A. Nilsson, L. G. M. Pettersson, and J. K. Nørskov, *Chemical bonding at surfaces and interfaces* (Elsevier, Amsterdam; Oxford, 2008), URL http://site.ebrary.com/id/10190879.

[4] D. J. Doren and J. C. Tully, Langmuir **4**, 256 (1988), URL http://dx.doi.org/10.1021/la00080a004.

[5] D. J. Doren and J. C. Tully, J. Chem. Phys. **94**, 8428 (1991), URL http://scitation.aip.org/content/aip/journal/jcp/94/12/10.1063/1.460076.

[6] M. Bowker, J. Phys.: Condens. Matter **22**, 263002 (2010), URL http://iopscience.iop.org/0953-8984/22/26/263002.

[7] J. B. Taylor and I. Langmuir, Phys. Rev. **44**, 423 (1933), URL http://link.aps.org/doi/10.1103/PhysRev.44.423.

[8] M. Bowker, Langmuir **7**, 2534 (1991), URL http://pubs.acs.org/doi/abs/10.1021/la00059a023.

[9] M. Dell'Angela, T. Anniyev, M. Beye, R. Coffee, A. Föhlisch, J. Gladh, T. Katayama, S. Kaya, O. Krupin, J. LaRue, et al., Science **339**, 1302 (2013), URL http://www.sciencemag.org/content/339/6125/1302.

[10] M. Beye, T. Anniyev, R. Coffee, M. Dell'Angela, A. Föhlisch, J. Gladh, T. Katayama, S. Kaya, O. Krupin, A. Møgelhøj, et al., Phys. Rev. Lett. **110**, 186101 (2013), URL http://link.aps.org/doi/10.1103/PhysRevLett.110.186101.

[11] N. D. Lang, S. Holloway, and J. K. Nørskov, Surf. Sci. **150**, 24 (1985), URL http://www.sciencedirect.com/science/article/B6TVX-46SWV91-1CC/1/6da2ff9a376d4a1c4db2192ca0ba9b69.

[12] F. M. Hoffmann, M. D. Weisel, and C. H. F. Peden, Surf. Sci. **253**, 59 (1991), URL http://www.sciencedirect.com/science/article/pii/003960289190581C.

[13] H. Pfnür, P. Feulner, and D. Menzel, J. Chem. Phys. **79**, 4613 (1983), URL http://scitation.aip.org/content/aip/journal/jcp/79/9/10.1063/1.446378.

[14] W. F. Schlotter, J. J. Turner, M. Rowen, P. Heimann, M. Holmes, O. Krupin, M. Messerschmidt, S. Moeller, J. Krzywinski, R. Soufli, et al., The Review of Scientific Instruments **83**, 043107 (2012), URL http://scitation.aip.org/content/aip/journal/rsi/83/4/10.1063/1.3698294.

[15] A. Föhlisch, W. Wurth, M. Stichler, C. Keller, and A. Nilsson, J. Chem. Phys. **121**, 4848 (2004), URL http://scitation.aip.org/content/aip/journal/jcp/121/10/10.1063/1.1778380.

[16] *See Supplemental Material for details.*

[17] J. Gladh, T. Hansson, and H. Öström, Surf. Sci. **615**, 65 (2013), URL http://www.sciencedirect.com/science/article/pii/S0039602813001404.

[18] M. Bonn, C. Hess, S. Funk, J. H. Miners, B. N. J. Persson, M. Wolf, and G. Ertl, Phys. Rev. Lett. **84**, 4653 (2000), URL http://link.aps.org/doi/10.1103/PhysRevLett.84.4653.

[19] S. Funk, M. Bonn, D. N. Denzler, C. Hess, M. Wolf, and G. Ertl, J. Chem. Phys. **112**, 9888 (2000), URL http://link.aip.org/link/?JCP/112/9888/1.

[20] H. Öberg, J. Gladh, H. Ogasawara, A. Nilsson, L. G. M. Pettersson, and H. Öström, manuscript (2015).

[21] M. Bonn, S. Funk, C. Hess, D. N. Denzler, C. Stampfl, M. Scheffler, M. Wolf, and G. Ertl, Science **285**, 1042 (1999), URL http://www.sciencemag.org/cgi/content/abstract/285/5430/1042.

[22] H.-J. Freund, G. Meijer, M. Scheffler, R. Schlögl, and M. Wolf, Angew. Chem. Int. Ed. **50**, 10064 (2011), URL http://onlinelibrary.wiley.com/doi/10.1002/anie.201101378/abstract.

[23] M. Lisowski, P. A. Loukakos, U. Bovensiepen, J. Sthler, C. Gahl, and M. Wolf, Applied Physics A **78**, 165 (2004),URL http://link.springer.com/article/10.1007/s00339-003-2301-7.

[24] S. I. Anisimov and B. Rethfeld, in *Nonresonant Laser-Matter Interaction (NLMI-9)*, edited by V. I. Konov and M. N. Libenson (SPIE, St. Petersburg, Russia, 1997), vol. 3093, pp. 192–203, URL http://link.aip.org/link/?PSI/3093/192/1.

[25] M. Brandbyge, P. Hedegård, T. F. Heinz, J. A. Misewich, and D. M. Newns, Phys. Rev. B **52**, 6042 (1995), URL http://link.aps.org/doi/10.1103/PhysRevB.52.6042.

[26] H. Öström, H. Öberg, H. Xin, J. LaRue, M. Beye, M. Dell′Angela, J. Gladh, M. L. Ng, J. A. Sellberg, S. Kaya, et al., Science **347**, 978 (2015), URL http://www.sciencemag.org/content/347/6225/978.

[27] J. Wellendorff, K. T. Lundgaard, A. Møgelhøj, V. Petzold, D. D. Landis, J. K. Nørskov, T. Bligaard, and K. W. Jacobsen, Phys. Rev. B **85**, 235149 (2012), URL http://link.aps.org/doi/10.1103/PhysRevB.85.235149.

[28] M. Baer, *Theory of Chemical Reaction Dynamics*, vol. 4 (CRC Press, 1985).

[29] A. Föhlisch, M. Nyberg, J. Hasselström, O. Karis, L. G. M. Pettersson, and A. Nilsson, Phys. Rev. Lett. **85**, 3309 (2000), URL http://link.aps.org/doi/10.1103/PhysRevLett.85.3309.

[30] L. G. M. Pettersson and A. Nilsson, Top Catal **57**, 2 (2014), URL http://link.springer.com/article/10.1007/s11244-013-0157-4.

[31] C. Stampfl and M. Scheffler, Phys. Rev. B **65**, 155417 (2002), URL http://link.aps.org/doi/10.1103/PhysRevB.65.155417.

[32] K. Kostov, H. Rauscher, and D. Menzel, Surf. Sci. **278**, 62 (1992), URL http://www.sciencedirect.com/science/article/pii/003960289290584S.

[33] M. Föhlisch, A. and, P. Bennich, L. Triguero, J. Hasselström, O. Karis, L. G. M. Pettersson, and A. Nilsson, J. Chem. Phys. **112**, 1946 (2000), URL http://scitation.aip.org/content/aip/journal/jcp/112/4/10.1063/1.480773.

[34] P. S. Bagus, K. Hermann, and C. W. Bauschlicher, Jr, J. Chem. Phys. **80**, 4378 (1984), URL http://scitation.aip.org/content/aip/journal/jcp/80/9/10.1063/1.447215.